

Strong radiation force induced in two-dimensional photonic crystal slab cavitiesHideaki Taniyama,^{1,3,*} Masaya Notomi,^{1,3} Eiichi Kuramochi,^{1,3} Takayuki Yamamoto,^{1,2,3} Yutaka Yoshikawa,^{2,3} Yoshio Torii,^{2,3} and Takahiro Kuga^{2,3}¹*NTT Basic Research Laboratories, NTT Corporation, 3-1 Morinosato-Wakamiya, Atsugi 243-0198, Japan*²*Institute of Physics, University of Tokyo, Komaba 3-8-1, Meguro-ku, Tokyo 153-8902, Japan*³*CREST, Japan Science and Technology Agency, 4-1-8 Honcho, Kawaguchi, Saitama 332-0012, Japan*

(Received 12 May 2008; published 31 October 2008)

Radiation force induced by an electromagnetic field stored in a two-dimensional photonic crystal slab is examined. We considered two different types of photonic crystal cavities, namely, double-layer slab cavity structures and air-slot cavity structures. With double-layer structures, induced force is attractive or repulsive depending on the spatial symmetry of the stored electromagnetic field profile. For air-slot structures, we showed that a horizontal attractive force is induced between slabs, and it could be stronger than that for double-layer structures in the case considered here. The induced force on a photonic crystal slab is so strong that it can be detected experimentally with the microelectromechanical systems technique. A simple physical model based on a coupled-resonator well describes these results.

DOI: [10.1103/PhysRevB.78.165129](https://doi.org/10.1103/PhysRevB.78.165129)

PACS number(s): 42.70.Qs, 42.79.Gn

I. INTRODUCTION

Optical microcavities are attracting considerable research interest, and great progress has been made on the quality factor (Q) of ultrasmall optical resonators, such as photonic crystal (PC) slab^{1,2} and whispering-gallery cavities.³ These resonators exhibit an extremely high Q with a very small cavity volume, which suggest a large enhancement of the optical nonlinear effect.^{4,5} There has also been a great interest in detecting and using radiation force as a result of studies on the van der Waals and Casimir forces.^{6–11} The development of micromechanical and nanoelectromechanical system (NEMS) techniques has greatly improved the sensitivity of force measurement, and these have become a useful and essential technique. The radiation force-induced mechanical oscillation of an optical microcavity is experimentally and theoretically investigated.^{12–14} Recently, some studies reported that light can also exert a large force if confined to small structures,^{15,16} and the optical manipulation of mechanical structures is being studied extensively.

Recently, we proposed double-layer two-dimensional photonic crystal slab (DL-PCS) cavities and showed that resonant frequency can be controlled by changing the separation between two slabs.⁵ The amount of change in resonant frequency is very large and cannot be achieved by other physical phenomena. This is because despite the fact that many researchers are trying to control resonant frequency by changing the refractive index of a given medium, the change in refractive index induced by an optical nonlinear effect is very small.^{17,18} Our study has shown that DL-PCS, which is a special cavity design, can achieve a large frequency change without changing the refractive index. The underlying physics of the frequency change by DL-PCS is based on the optomechanical coupling of cavities. Furthermore, we demonstrated frequency conversion by dynamically shifting their separation.⁴ With DL-PCS, we have also suggested that a strong radiation force is induced between two slabs. These two phenomena are closely related, and in terms of energy conservation, they can be considered to constitute mechani-

cal to optical energy conversion. The suggested concept is interesting from both basic physical point of view and as regards to practical applications. That paper was the first to indicate the beginning of physically new schemes of optics offering the potential for the efficient conversion of mechanical energy to optical energy.

In our previous study, we reported a DL-PCS structure with efficient energy conversion that had a very high Q and a small mode volume. Some types of optical cavities have been reported including photonic crystal slab cavities^{1,2} and toroidal cavities.³ Of these cavity structures, the reported Q factor of a toroid microcavity is about 10^8 , which is much higher than that of PC slab cavities. However, its effective mode volume is $100(\lambda/n)^3$, which is much larger than that of PC slab cavities. The Q factor of photonic crystal has recently achieved a value of around 10^6 and the effective mode volume is ~ 1 .¹⁹ This means that the electromagnetic (EM) field is confined within an extremely small volume in PC cavities and the energy concentration and field strength are much stronger than those in toroid cavities. For this reason, we can expect a large optical nonlinear effect with low energy in PC slab cavities. This is why the PhC slab cavity intrigues many researchers. A strong radiation force can also be expected for PC cavities because they have a strong electromagnetic field concentration in a very small volume.

In this paper, we analyze the radiation force between photonic crystal slabs induced by an electromagnetic wave stored in a cavity. Two types of cavity structures are considered in this paper. One is a double-layer photonic crystal cavity and the other is an air-slot (AS) photonic crystal cavity. We use the three-dimensional (3D) finite-difference time-domain (FDTD) method to simulate the time evolution of an electromagnetic field. The paper is organized as follows. In Sec. II we briefly describe the theory of radiation force. We describe the two types of cavity structure and their characteristics in Sec. III. Simple mathematical picture of these cavities is provided in Sec. IV.

II. METHOD

The 3D FDTD method is used to calculate the resonant frequency, the field profile, and its time evolution process. Q is obtained by an exponential fit of the electromagnetic energy decay, and the resonant frequency is obtained by a Fourier transform of the field. We use two different methods to calculate the radiation force of an EM field. One employs the differentiation of the energy U by the slab separation d . Here,

$$F = -\frac{\partial U}{\partial d}, \quad (1)$$

where U is the stored EM field energy. This relation is based on the energy conservation law in fundamental physics. The EM field energy stored in a cavity is calculated as $\hbar\nu$, where ν is the resonant frequency of the cavity. This is an approximation whereby all contributory field frequencies have resonant frequency. This means that the spectral width of the resonance is disregarded. Because the Q factor of the cavity considered here is very large, this approximation can be justified.

The other method involves the force derived from the energy-momentum tensor (EMT) of the stored EM field.²⁰⁻²⁵ It is based on a microscopic description of the electromagnetic field. An electromagnetic field imposes a force on dielectric materials. This force is calculated as a Lorentz force, $F = e(\mathbf{E} + \mathbf{v} \times \mathbf{B})$. A Maxwell equation is used to calculate the radiation force, which acts on a medium of volume V , as follows:

$$F_\alpha = \int_V \sum_\beta \frac{T_{\alpha\beta}}{\partial x_\beta} dV, \quad (2)$$

where α and β indicate x , y , and z , and $T_{\alpha\beta}$ is the EMT defined as

$$T_{\alpha\beta} = \epsilon E_\alpha E_\beta + \mu H_\alpha H_\beta - \frac{1}{2}[\epsilon E_\gamma E_\gamma + \mu H_\gamma H_\gamma]. \quad (3)$$

Using the divergence theorem the volume integration in Eq. (2) is reduced to the integration over the surface S ,

$$F_\alpha = \oint_S \mathbf{T}_\alpha \cdot d\mathbf{s}. \quad (4)$$

If the EM field is strongly confined in a cavity, namely, there is no leak, a radiation force calculated by both Eqs. (1) and (2) must give the same result. However, there is generally a finite fraction of the EM field that radiates outward from a cavity. Because an EM field has momentum, this leaked field causes a counteraction on a PC cavity structure. This means that a finite amount of radiation loss from a cavity will cause recoil on the slab and this force is not included in Eq. (2). The EM field momentum P_{field} within a volume V is written as

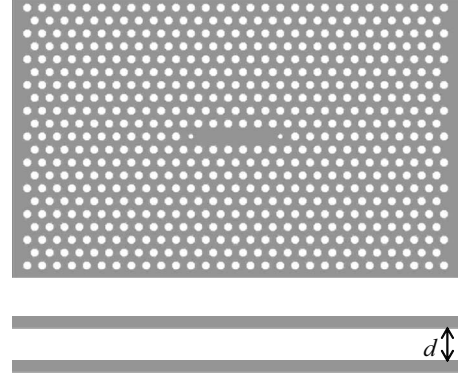


FIG. 1. Double-layer of five-hole defect photonic crystal cavity. The cavity consists of five missing holes with shifted side holes. Two slabs are located with a separation d . The thickness of each slab t is 105 nm.

$$P_{\text{field}} = \frac{1}{c^2} \int_V \mathbf{E} \times \mathbf{H}, \quad (5)$$

and a recoil force is obtained by a time differentiation of P_{field} . The expression we used in Eq. (5) is Abraham's momentum.^{24,26-28} The total force, which acts on a materials, is expressed as a sum of these two terms,

$$f_{\text{total}} = F - \frac{\partial P_{\text{field}}}{\partial t}. \quad (6)$$

III. RADIATION FORCE ON SLABS

A. Double-layer photonic crystal slab cavity

We study two types of cavity structures. The first structure presented in this subsection is DL-PCS, which we reported in our previous paper.⁴ We calculate the radiation force induced by an electromagnetic field stored in double-layer two-dimensional PC slabs. The structure used for the calculation is shown schematically in Fig. 1. It consists of two hexagonal air-hole Si PC slabs with identical five-hole cavities and shifted end-hole positions.²⁹ Two slabs are separated by a distance d , the thickness of each slab is $t=105$ nm, the lattice constant is $a=420$ nm, and the radius $r=115.5$ nm. A single slab has a Q factor of 220 000 with a mode volume of $0.12 \mu\text{m}^3$ for $\lambda=1580$ nm.

Let us consider two PC slab cavities with the same resonant wavelength. When the two slabs are separated sufficiently, mode coupling can be ignored; but when the two slabs are close together, $d \rightarrow 0$, the fundamental modes of each layer couple, and this constitutes the even-parity and odd-parity modes. Within these modes, the fundamental mode of the entire structure always has even parity in the vertical direction. Figure 2 shows mode profiles of (a) the even-parity and (b) odd-parity modes. The horizontal profiles of both modes are almost the same, which is similar to a single isolated slab cavity.

Figure 3 shows the Q -factor characteristics of the even and odd modes as a function of slab separation d . The Q factor of an even mode remains high when the slab separa-

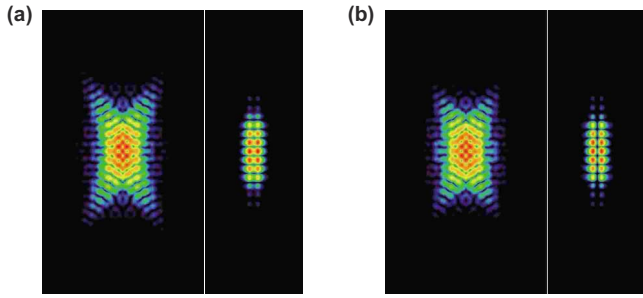


FIG. 2. (Color online) Mode: top and side views of DL-PCS cavity modes. (a) is the even mode and (b) is the odd mode in the vertical direction.

tion becomes small but the Q of an odd mode decreases greatly. This is because an even mode is a fundamental mode for a PCS cavity of thickness $2t$, but an odd mode is above the light line of air, which means a radiation mode. We also found that modal volume does not depend on the separation. Figure 4 shows the resonant wavelength characteristics of the even and odd modes as a function of the slab separation d . There is a great variation in the resonant wavelengths of the two modes and the amount of change is almost the same for both.

As is intuitively expected from the symmetric nature of the mode profile, because the field profile of the even and odd modes are horizontally symmetric or antisymmetric, the radiation force acts only vertically. To calculate the radiation force on a slab, an EMT is integrated over the surface of the slab using Eq. (4). The calculated value of the force is normalized for a stored EM field energy of 1 pJ. Although the force decays as a function of time, the normalized force is nearly constant in time. The induced force is attractive for the even mode and repulsive for the odd mode. Figures 5 and 6 show the strength of the force acting on the slabs for the even and odd modes, respectively. The results obtained with Eqs. (1) and (2) are shown in the figures. The results indicate that the induced force is large so that it can be practically observed. The radiation force obtained here does not depend

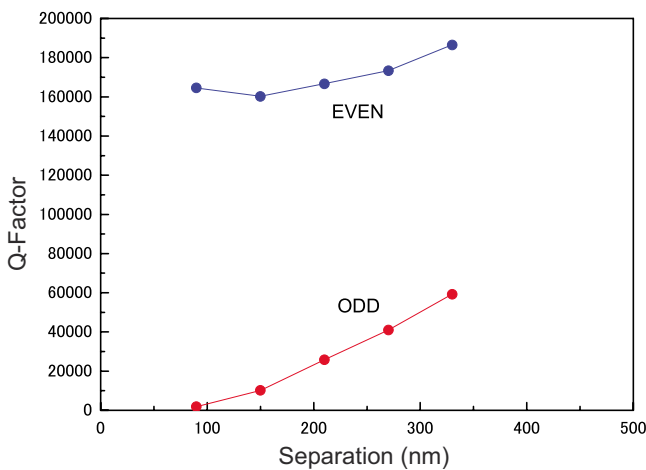


FIG. 3. (Color online) Q factor of double-layer cavities as a function of the separation of the two layers. The solid and open circles indicate the even and odd modes, respectively.

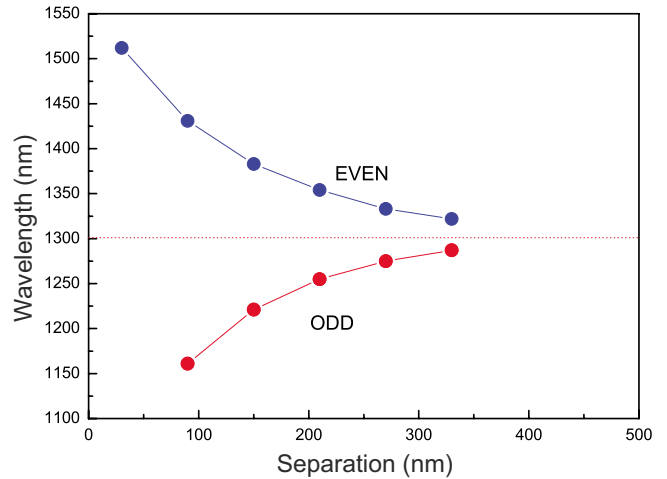


FIG. 4. (Color online) Resonant wavelength of double-layer cavities as a function of the separation of the two layers. The solid and open circles indicate the even and odd modes, respectively. The horizontal dotted line around 1300 nm indicates the resonant mode of an isolated slab cavity.

on the Q factor of the cavity. An extremely high Q is essential for this practical observation, and PC slabs offer the possibility of achieving such a high Q factor.³⁰ As shown here, a large change in the resonant wavelength while maintaining a high Q is an advantage of this structure that has not been previously predicted. Although it requires mechanical control of the structural parameters, the separation of the two slabs, a large amount of wavelength change, and a high Q are still attractive and even practically valuable.

For the even mode, the results calculated with the two methods are in good agreement, which is reasonable in terms of understanding the physical origin of the radiation force. However, for the odd mode, the two methods give slightly different values. The reason for this difference can be understood by considering the radiation loss of the EM field. The Q factor of the odd mode is much lower than that of the even mode as shown in Fig. 2. This means the radiation loss of the

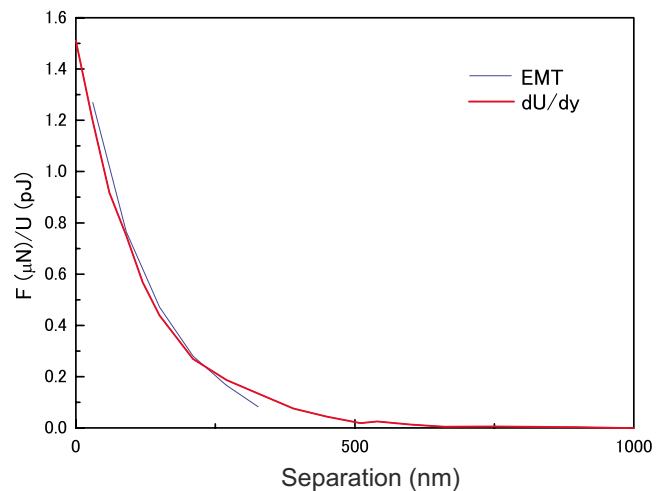


FIG. 5. (Color online) Radiation force of even mode. The solid circles are energy-momentum tensor results.

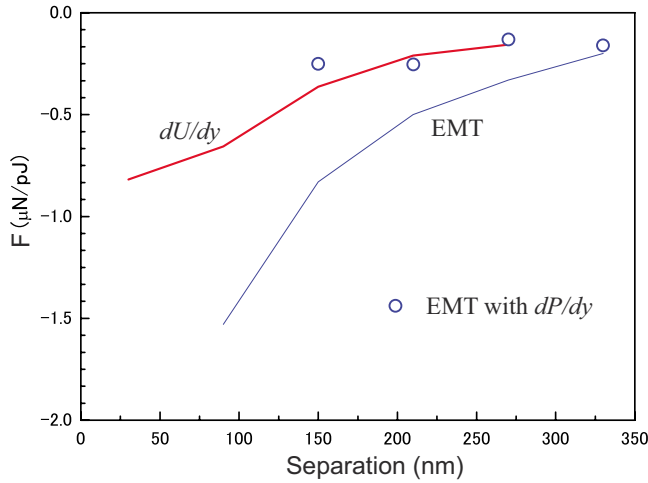


FIG. 6. (Color online) Radiation force of odd mode obtained with Eqs. (1) and (2). The open circles are EMT results including the effect of the field momentum term.

odd mode cannot be ignored. A reduction in the field momentum stored in a cavity means an outward flow of momentum, and the difference between the two results is attributed to the recoil of the radiated field. To confirm this conjecture, we determine the recoil force on slabs as the reaction of the leaking electric-field momentum, which we calculate from the temporal differentiation of the field momentum stored in a cavity, dP_{field}/dt . The results are shown by open circles in Fig. 6. As shown in the figure, the result agrees well with that of Eq. (1). For the even mode, the results without recoil agree well because the Q factor is sufficiently high and radiation can be ignored. The same analysis is performed for an even mode of the DL-PCS cavity with width-modulated photonic waveguide cavities.⁵ The cavity has an extremely high- Q cavity as already reported. The change in resonant wavelength as a function of slab separation is almost the same with the defect cavity described above. As a result of these characteristics, the same amount of radiation force is obtained. This means that the radiation force induced between slabs is independent of the Q factor of the optical resonator.¹⁶

B. Air-slot photonic crystal slab cavity

The second type of cavity structure is an AS cavity as shown schematically in Fig. 7. The structure is based on that of the width-modulated photonic waveguide cavity, which is designed as a part of a waveguide with the positions of some holes shifted outward.^{4,30} In this cavity, the EM field is confined in the cavity by both the photonic band gap and the waveguide mode gap. The structure we considered has a linear air slot of width d in the center of the width-modulated photonic waveguide cavity. Even with this air slot, the cavity still has a small modal volume $V_m \sim 1$. A feature of this structure is the air slot in the center of the cavity where atoms can be trapped and interact with a strong electromagnetic field.³¹ The lattice constant $a=420$ nm, the hole radius $r=0.257a$, and $t=396$ nm. The resonant wavelength of a cavity as a function of separation d is calculated, and the result is shown

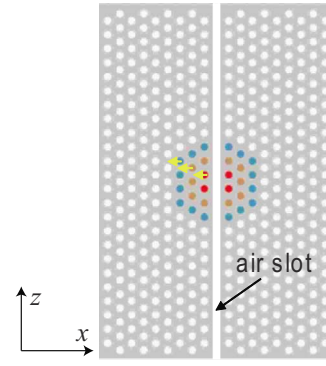


FIG. 7. (Color online) Air-slot cavity. The colored side holes have the same radius with their position shifted outward.

Fig. 8. The DL-PCS results are also shown in the figure. With the AS cavity, the change in the resonant wavelength is large and the amount of variation is almost the same as with DL-PCS. However, they behave differently. In particular, for a small separation <100 nm, the change in the AS cavity is steeper and larger than that with DL-PCS. For a separation larger than 100 nm, the resonant wavelength change is very small, while the change for DL-PCS is gradual. The total amount of change in the resonant wavelength is similar for both structures. The Q factor for a cavity with $d=0$ is about 10^7 and remains larger than 10^5 for a separation smaller than $d=100$ nm.³¹ The difference between the characteristics is attributed to the physical origin of the cavity mode. With DL-PCS, the structure still has a cavity in each slab for a large slab separation. However, the AS structure does not retain its cavity property with a large separation. The resonant mode around 1500 nm for a large separation has a small Q , which is thought to be the slab's surface mode.

For an AS cavity, we consider a fundamental mode. Because the mode we consider has a vertically symmetric mode profile, only horizontal radiation force is induced. While at the upper and lower surfaces, only the tensor components T_{xy} contribute to the net radiation force and the T_{xx} component contributes on the AS surface (see Fig. 9). The calculated

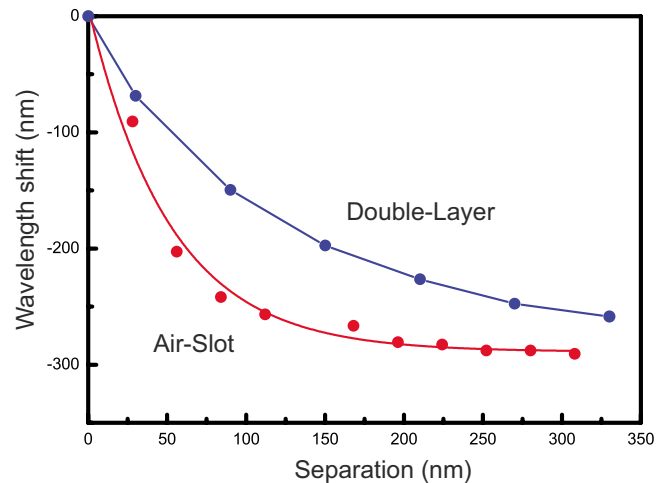


FIG. 8. (Color online) Calculated resonant wavelength of air-slot cavities (red) and of DL-PCS cavities (blue).

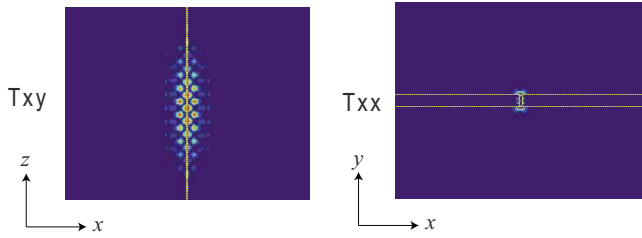


FIG. 9. (Color online) T_{xx} and T_{xy} components of EM tensor.

results are shown in Fig. 10. The radiation force reaches twice that of DL-PCS for a small separation. This strong radiation field is induced by the large electromagnetic field distribution in the air-slot region.³¹ The force decreases rapidly and becomes weaker than that of DL-PCS for a separation wider than 40 nm.

IV. SIMPLE NUMERICAL MODEL OF CAVITIES

The radiation force obtained here is much stronger than has been yet predicted. Microscopically this force is induced as a result of the multiple scattering of the electromagnetic field in the cavity, which bounces back and forth. There is a similar multiple-scattering phenomenon in a Fabry-Perot resonator. Is it possible that a Fabry-Perot resonator could also provide to such a strong radiation force or is it specific to the type of cavities considered here? To answer this question, we consider simple numerical models of resonators and estimate the radiation force. We consider two numerical models, namely, the Fabry-Perot resonator and a coupled-cavity model (see Fig. 11).

Let us assume a Fabry-Perot resonator that consists of two parallel media with a cavity between them. The wavelength of an optical field stored in the cavity can be obtained as follows. The reflection coefficient of one interface is generally described as

$$r = \frac{\beta(k) + ik}{-\beta(k) + ik} = e^{(i/2)\alpha(k)}, \tag{7}$$

where k is the wave number, $\alpha(k)$ is the phase shift of a field in a reflection at an interface, and $\beta(k)$ is the decay rate of an

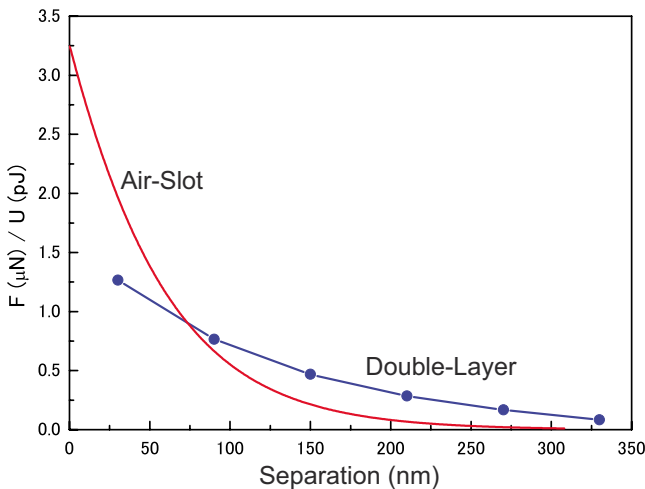


FIG. 10. (Color online) Radiation force of air-slot cavities compared with that of double-layer cavities.

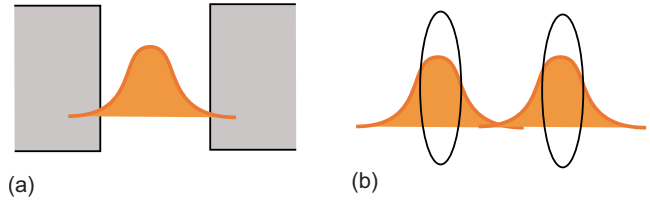


FIG. 11. (Color online) (a) is a schematic of the Fabry-Perot resonator model, which has a cavity between half-infinite dielectric media. (b) is a schematic of a coupled cavity model where two cavities couple through an evanescent field.

evanescent field in the medium. We assume that the field is completely reflected, and so leakage can be ignored. From Eq. (7), an eigenmode equation for a Fabry-Perot resonator is represented as

$$2kd + \alpha(k) = 2\pi n, \tag{8}$$

where d is the separation between the two media, kd is the phase shift between two interfaces, and n is a positive integer. With a small separation limit, we obtain an approximated equation as

$$k = \frac{ck_0}{2d + c}, \tag{9}$$

where $c = \partial\alpha / \partial k$. Equation (9) gives the resonant wavelength as a function of the separation of the two media. The equation gives a shorter resonant wavelength for a smaller separation.

For a coupled-cavity model, the resonant wavelength can be calculated as a function of the coupling strength of two cavities. We assume that two isolated cavities have same resonant wavelength. When two cavities are close together, the coupling between the two cavities becomes strong and the degenerated eigenmode begins to separate into two modes as a result of the coupling. Here,

$$\hbar\omega = \hbar\omega_0 \pm \alpha. \tag{10}$$

With the coupled-cavity model, the antibonding mode exhibits similar eigenmode dependence as a function of separation. The evanescent coupling between cavities decreases exponentially with distance. The coupling strength is calculated with the usual technique as the overlap integral of the evanescent field between two cavities. The resonant wavelengths calculated with these two models are shown in Fig. 12. The parameters used in the calculation assumed that the resonant wavelength for $d=0$ is 1100 nm. The shorter wavelength mode between two coupled-cavity modes and the eigenmode of the Fabry-Perot model are shown in the figure. This shows that the two models have different wavelength characteristics as a function of separation. A notable difference can be seen for the small separation region near $d=0$. Although the coupled-cavity model shows a continuous decrease in the resonant wavelength, the Fabry-Perot model shows saturation in the resonant wavelength near $d=0$. This occurs because, with the Fabry-Perot model, the penetration of an evanescent field into the medium becomes large in this region. The difference in the physical nature of the two models is

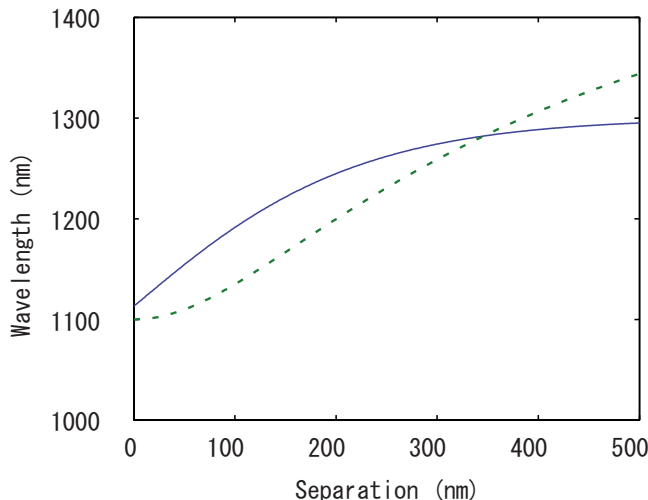


FIG. 12. (Color online) Resonant wavelength calculation with Fabry-Perot (dashed line) and coupled-resonator (solid line) models.

clearly recognized when we calculate the radiation force. The result is shown in Fig. 13. For a coupled-resonator model, a radiation force becomes very large when d approaches zero. However, for a Fabry-Perot model, a radiation field reaches its maximum value for a separation of around 150 nm and becomes weak as d approaches zero. It is clear that the DL-PCS cavity can be explained with the coupled-cavity model. It is also reasonable for the AS cavity to be explained by the coupled-cavity model because the Fabry-Perot resonator model does not exhibit to the strong radiation force found with proposed structures. This is the physical mechanics, whereby the DL-PCS and AS cavities provide a strong radiation field as indicated here.

V. CONCLUSION

We analyzed the radiation force on slabs induced by an electromagnetic field stored in cavities and showed that the induced force is so strong that it can be measured using the

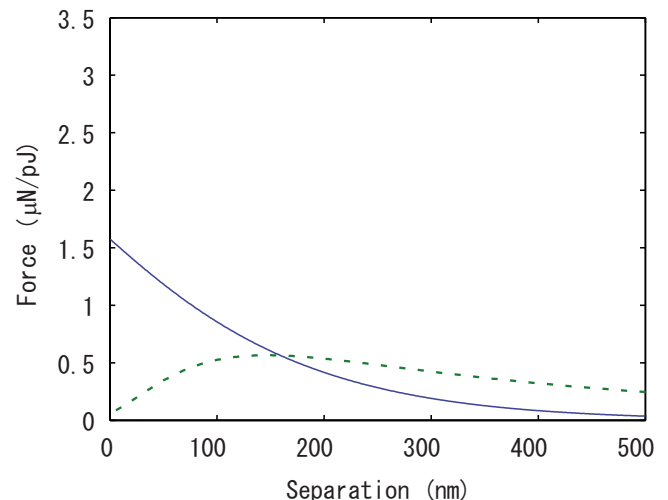


FIG. 13. (Color online) Radiation force calculation with Fabry-Perot (dashed line) and coupled-resonator (solid line) models.

recently developed NEMS technique. The structure also exhibits a large wavelength change for a small change in separation, which is not independent of the strong radiation force. The predicted strength of the radiation force does not depend on the Q factors; however, a sufficiently high Q is preferable for two reasons. The measurement must be performed within the lifetime of the stored EM field, and the radiation field caused by a low Q leads to a recoil and reduces the radiation force acting on the slabs. For the above two reasons, a sufficiently high Q factor is required for practical experiments. Extremely high- Q values have been reported for PCS cavities.³⁰ PCS cavities are generally very small. The structures proposed here are very promising for measuring radiation force and is also a candidate as a future optical elements in, for example, a wavelength controller, an optical sensor, and an energy converter.

ACKNOWLEDGMENTS

The authors thank Y. Tokura for his encouragement throughout this work. This work was supported by JST-CREST.

*tani@will.brl.nitt.co.jp

¹Y. Akahane, T. Asano, B. Song, and S. Noda, *Nature (London)* **425**, 944 (2003).

²B. S. Song, S. Noda, T. Asano, and Y. Akahane, *Nature Mater.* **4**, 207 (2005).

³D. K. Armani, T. J. Kippenberg, S. M. Spillane, and K. J. Vahala, *Nature (London)* **421**, 925 (2003).

⁴M. Notomi, H. Taniyama, S. Mitsugi, and E. Kuramochi, *Phys. Rev. Lett.* **97**, 023903 (2006).

⁵M. Notomi and S. Mitsugi, *Phys. Rev. A* **73**, 051803(R) (2006).

⁶H. B. G. Casimir, *Proc. K. Ned. Akad. Wet.* **51**, 793 (1948).

⁷E. M. Lifshitz, *Sov. Phys. JETP* **2**, 73 (1956).

⁸P. F. Cohadon, A. Heidmann, and M. Pinard, *Phys. Rev. Lett.* **83**, 3174 (1999).

⁹H. B. Chan, V. A. Aksyuk, R. N. Kleiman, D. J. Bishop, and

Federico Capasso, *Science* **291**, 1941 (2001).

¹⁰T. Carmon, H. Rokhsari, L. Yang, T. J. Kippenberg, and K. J. Vahala, *Phys. Rev. Lett.* **94**, 223902 (2005).

¹¹P. T. Rakich, M. A. Popovič, M. Soljačić, and E. P. Ippen, *Nat. Photonics* **1**, 658 (2007).

¹²H. Rokhsari, T. J. Kippenberg, T. Carmon, and K. J. Vahala, *Opt. Express* **13**, 5293 (2005).

¹³M. L. Povinelli, M. Loncar, M. Ibanescu, E. J. Smythe, S. G. Johnson, F. Capasso, and J. D. Joannopoulos, *Opt. Lett.* **30**, 3042 (2005).

¹⁴M. L. Povinelli, S. G. Johnson, M. Loncar, M. Ibanescu, E. J. Smythe, F. Capasso, and J. D. Joannopoulos, *Opt. Express* **13**, 8286 (2005).

¹⁵H. Taniyama, M. Notomi, E. Kuramochi, T. Yamamoto, Y.

- Yoshikawa, Y. Torii, and T. Kuga, in Proceedings of the Photonic and Electromagnetic Crystal Structures (PECS VII), Monterey, 8–10 April 2007, p. B-55.
- ¹⁶M. Eichenfield, C. P. Michael, R. Perahia, and O. Painter, *Nat. Photonics* **1**, 416 (2007).
- ¹⁷M. Notomi, A. Shinya, S. Mitsugi, G. Kira, E. Kuramochi, and T. Tanabe, *Opt. Express* **13**, 2678 (2005).
- ¹⁸T. Tanabe, M. Notomi, S. Mitsugi, A. Shinya, and E. Kuramochi, *Opt. Lett.* **30**, 2575 (2005).
- ¹⁹E. Kuramochi, M. Notomi, S. Mitsugi, A. Shinya, T. Tanabe, and T. Watanabe, *Appl. Phys. Lett.* **88**, 041112 (2006).
- ²⁰K. A. Milton, *Ann. Phys. (N.Y.)* **127**, 49 (1980).
- ²¹G. Plunien, B. Müller, and W. Greiner, *Phys. Rep.* **134**, 87 (1986).
- ²²M. Bordag, U. Mohideen, and V. M. Mostepanenko, *Phys. Rep.* **353**, 1 (2001).
- ²³A. Rodriguez, M. Ibanescu, D. Iannuzzi, F. Capasso, J. D. Joannopoulos, and S. G. Johnson, *Phys. Rev. Lett.* **99**, 080401 (2007).
- ²⁴J. D. Jackson, *Classical Electrodynamics*, 3rd ed. (Wiley, New York, 1998).
- ²⁵L. D. Landau, E. M. Lifshitz, and L. P. Pitaevskii, *Electrodynamics of Continuous Media*, 2nd ed. (Elsevier, Oxford, 1993).
- ²⁶J. P. Gordon, *Phys. Rev. A* **8**, 14 (1973).
- ²⁷I. Brevik, *Phys. Rep.* **52**, 133 (1979).
- ²⁸R. N. C. Pfeifer, T. A. Nieminen, N. R. Heckenberg, and H. Rubinsztein-Dunlop, *Rev. Mod. Phys.* **79**, 1197 (2007).
- ²⁹S. Mitsugi, A. Shinya, E. Kuramochi, M. Notomi, T. Tsuchizawa, and T. Watanabe, Proceedings of the 16th Annual Meeting of IEEE Lasers and Electro-Optics Society (LEOS '03), Tucson, Arizona, October 2003, Vol. 1, p. 214.
- ³⁰E. Kuramochi, M. Notomi, S. Mitsugi, A. Shinya, T. Tanabe, and T. Watanabe, Proceedings of the 18th Annual Meeting of the IEEE Lasers and Electro-Optics Society (LEOS '05), Sydney, Australia, October 2005, PD1.1.
- ³¹T. Yamamoto, M. Notomi, H. Taniyama, E. Kuramochi, Y. Yoshikawa, Y. Torii, and T. Kuga, *Opt. Express* **16**, 13809 (2008).